Strain tuning of excitons in monolayer WSe₂

Burak Aslan,[*] Minda Deng, and Tony F. Heinz

Department of Applied Physics, Stanford University, Stanford, California 94305, USA
and SLAC National Accelerator Laboratory, Menlo Park, California 94025, USA

We investigate excitonic absorption and emission in monolayer (1L) WSe₂ under tensile strain. We observe a redshift of 100 meV in the A exciton energy and a decrease of 25 meV in its estimated binding energy under 2.1% strain. Surprisingly, the linewidth of the A exciton decreases by almost a factor of two under strain, from 42 to 24 meV at room temperature. We explain this effect as the result of suppression of phonon-mediated exciton scattering channels. We show that such a suppression results from the relative shift under strain of a secondary valley in the conduction band that is nearly degenerate with the K valley where the A exciton is formed.

I. INTRODUCTION

Excitons dominate the optical spectra of atomically thin semiconducting transition metal dichalcogenides (TMDCs) due to their high binding energy and oscillator strength [1,2]. It is thus invaluable to understand them for many-body physics and fundamental studies on TMDCs. The ability to tune them is, moreover, very valuable for optoelectronic applications. Recent studies have demonstrated the tunability of optical gaps and excitonic binding energies by 10s of meV via external control such as electrical gating, magnetic fields, and dielectric screening [3–7]. Strain tuning, another external control, has been repeatedly employed to engineer the optical spectra of monolayer (1L) TMDCs [8–15]. Redshifts of more than 400 meV in the optical gap [8], indirect to direct gap transitions [10], and changes in the spectral linewidths via strain have been reported in TMDCs [11,12,15–17]. In contrast, the influence of strain tuning on their electrical (quasiparticle) band gaps or on excitonic binding energies has not yet been investigated. Moreover, the effect of strain on other optical fingerprints such as linewidth has yet to be modeled or fully understood.

II. STRAIN AS A PROBE

Strain can provide a means of probing the band structure of monolayers and the relative disposition of different minima in the conduction band (CB). 1L TMDCs are expected to possess direct gaps, but with indirect gaps only a few 10s to 100s of meV higher in energy [18–20]. Therefore, the optical and electrical properties of 1Ls may be strongly influenced by the exciton- and carrier-phonon scattering between valleys at room and elevated temperatures [19,21–23]. It has been proposed that tensile strain can alter the energy separation between the two states associated with the direct and indirect gaps, affecting the scattering rates [24–27]. Consequently, we expect that the altered energy separation under strain

may lead to observable fingerprints in the optical spectra of the material. In this manner, strain can provide a means of optically probing the indirect gap, which is difficult to probe by optical spectroscopy when its energy is very close to that of the direct gap.

III. METHODS

In this study, we apply uniaxial tensile strain to 1L WSe₂ and perform *in situ* optical absorption and photoluminescence (PL) spectroscopy (see the Supplemental Material (SM) sections S1 and S2 [28]). We extract the peak positions of the excitonic states and infer the changes in the excitonic binding energy induced by strain. We note a significant decrease in the spectral linewidths of the excitons. Despite the similar dependence of the material properties on strain, we observe quantitatively different line narrowing in 1L WS₂. We consider the strain dependence of the linewidth of the lowest lying exciton (KK or A exciton) and show that the different narrowing can be explained by reduced phonon-mediated intervalley scattering rate from the direct to the lowest lying indirect [KQ (also known as $K\Lambda$)] excitonic state. By making use of the strain dependence of the excitonic gaps and binding energies observed, we calculate the strain-dependent intervalley scattering rate within the deformation potential approximation. We then give an estimate for the separation between the KK and KQ excitons, which has been examined in recent studies [29–31]. It is important to note that we refer to the spin-allowed states with respect to the top of the K point in the valence band (VB) for the A exciton in this paper, which are higher and lower energy spin states of the K and Q valleys in CB, respectively [18].

IV. CHOICE OF MATERIALS

We focus our attention on WSe₂ and WS₂ due to their large VB spin-orbit coupling. This enables the ready observation of the ground state and the excited states of the A exciton without the complication of the presence of the relatively broad B exciton in the critical spectral range. Moreover, the relatively
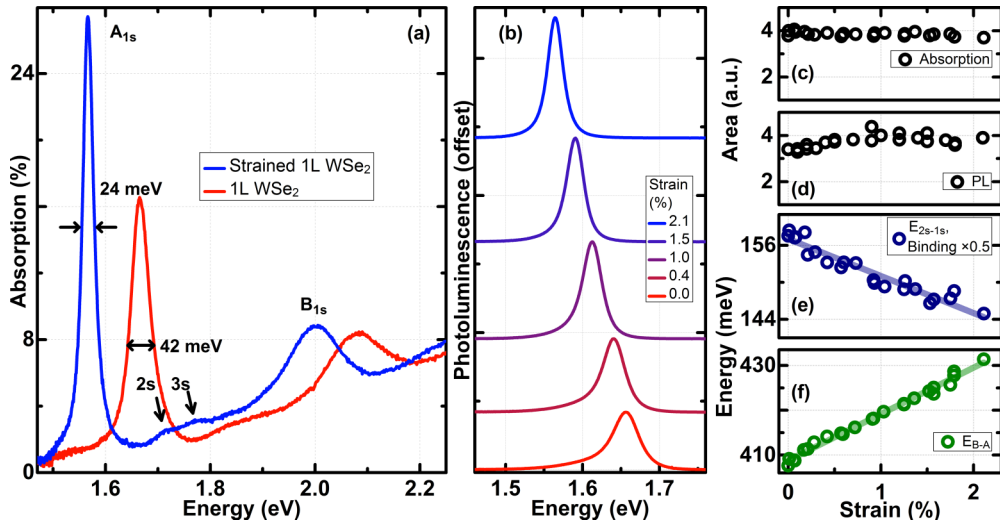
---

*oba2002@stanford.edu

FIG. 1. (a) Absorption spectra of 2.1% strained and unstrained 1L WSe$_2$. (b) Strain-dependent PL spectra of 1L WSe$_2$ (offset). Strain dependence of the strength of (c) absorption and (d) PL due to the A_{1s} exciton; (e) E_{2s-1s}, and A exciton binding energy; (f) E_{B-A}. Hollow circles are data points and solid lines are corresponding linear fits in (c)–(f).

small separation between the KK and KQ states makes the optical spectra of the excitons more sensitive to strain than systems such as MoS$_2$ and MoSe$_2$ which have been widely studied in strain-optics experiments [8,9,12–14,18].

V. STRAIN-TUNED ABSORPTION AND PL SPECTRA

We plot the effect of strain on the absorption and PL of 1L WSe$_2$ in Fig. 1. The absorption spectra show that the A exciton redshifts from 1.67 eV to 1.57 eV and B exciton redshifts from 2.08 eV to 2.00 eV as the strain increases from 0.0% to 2.1%. The strain-induced redshifts are far greater than the exciton linewidths, allowing the ready identification of the influence of strain. Strain-dependent PL spectra confirm the redshift of the A exciton, verifying that the emission and absorption originate from the same physical transition. The amplitudes of the absorption and PL peaks of the A exciton increase by about 75%. Surprisingly, all the features observed become narrower. Specifically, the linewidths of the A exciton absorption and emission peaks decrease from 42 to 24 meV for 2.1% strain. In addition to the strong 1s state of the exciton (A_{1s}), we are also able to observe the 2s (A_{2s}) and 3s (A_{3s}) excited states, which become more pronounced under strain. Despite the spectral narrowing, oscillator strengths of the A exciton absorption and PL peaks (integrated areas under the peaks) are found to be nearly insensitive to strain as shown in Fig. 1(c) and Fig. 1(d), respectively. (see SM Sec. S3 for more absorption spectra [28]).

VI. ANALYSIS

We analyze the strain-dependent absorption spectra and extract the peak positions of the excitons by fitting to Lorentzian lineshapes [1]. We plot the energy separations between the A_{2s} and A_{1s} (E_{2s-1s}), and B and A excitons (E_{B-A}) and their linear fits in Fig. 1(e) and Fig. 1(f), respectively. We obtain from the fit that E_{2s-1s} decreases by a rate of 6($\pm$1) meV/% strain from an unstrained value of 157($\pm$1) meV. We estimate

the change in the exciton binding energy as twice E_{2s-1s} and find that it decreases from 315($\pm$2) meV by 12($\pm$2) meV/% strain [1,4]. This corresponds to a decrease of 3.8($\pm$0.6)% per % strain. This is in good agreement with the calculations of the strain dependence of the exciton binding energy as arising from a decrease in the exciton reduced mass [32,33]. We note that these analyses assume that the binding energy scales linearly with the reduced mass. However, for a binding energy scaling as the reduced mass, for instance, to the power 0.3 [34], the experimental data would imply a rate of decrease of the reduced mass with strain ($>$10% per % strain) exceeding the predicted rate. A and B excitons redshift at different rates so that E_{B-A} increases from 409 meV by 10 meV/% strain mainly due to the increase in the splitting of the top of VB at the K point [35,36] (see SM Sec. S7 [28]).

We next consider the strain-dependent linewidths of the A and B excitons. In Fig. 2(a), we plot the linewidths for the absorption features in WSe$_2$ as well as WS$_2$. The linewidth of the A (B) exciton of WSe$_2$ decreases from 42 (170) meV at 0.0% strain to 24 (146) meV at 2.1% strain. We observe a quantitatively different narrowing for WS$_2$: The linewidth of its A (B) exciton decreases from 30 (127) meV at 0.0% strain to 24 (119) meV at 1.5% strain and remains nearly invariant around 24–25 meV up to 2.3% strain.

VII. DISCUSSION

A. Effect of strain on linewidths

Here, to discuss the surprising strain-driven decrease in the A exciton linewidth, we note that it is determined principally by three processes [22]: Radiative decay (γ_{rad}), intravalley scattering (KK to KK exciton-phonon scattering; γ_{KK-KK}), and intervalley scattering (KK to KQ exciton-phonon scattering; γ_{KK-KQ}) rates. We may disregard the KK to KK' and KK to ΓK intervalley scattering processes, since their rates are understood to be relatively low, mainly due to the relatively small deformation potentials of the associated scattering mechanisms [19,22]. Let us now consider the effect
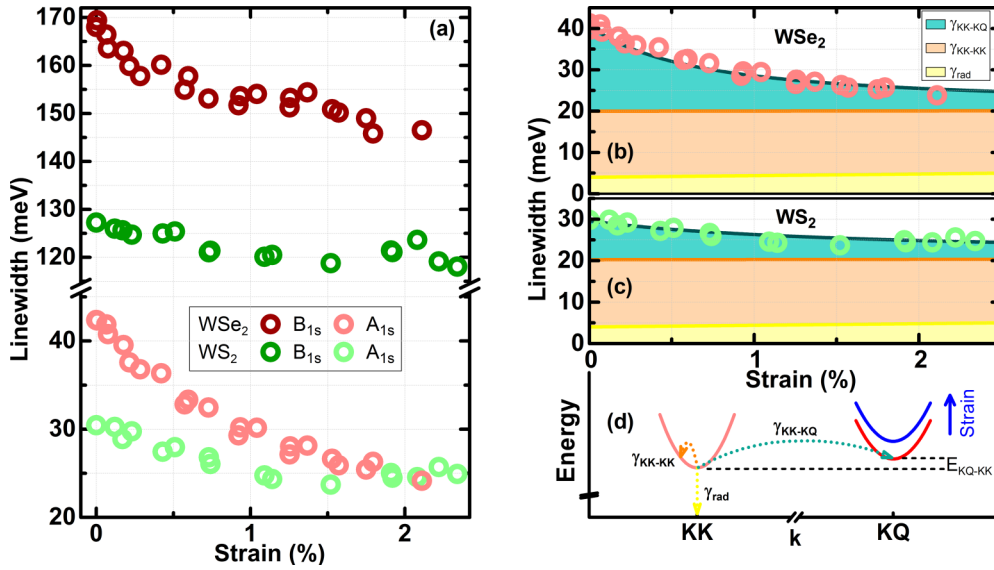
FIG. 2. (a) Experimentally measured strain dependence of the total linewidths of the A and B excitons in 1L WSe$_2$ and WS$_2$. Strain dependence of the extracted homogeneous linewidths and calculated contributions to the A exciton linewidth in 1L (b) WSe$_2$ and (c) WS$_2$ (see SM Sec. S8 [28]). The heights of the colored areas between the solid lines represent respectively the contributions from the radiative decay $\gamma_{\rm rad}$ (yellow), intravalley exciton-phonon scattering γ_{KK-KK} (orange), and intervalley exciton-phonon scattering γ_{KK-KQ} (turquoise). (d) Schematic representation of the line broadening mechanisms and the strain dependence of the relative energy levels of KQ and KK states.

of strain on these contributions. First, $\gamma_{\rm rad}$ of 1L WSe$_2$ and MoS$_2$ has been calculated to increase by about 10% per % strain [32]. We assume the same trend for WSe$_2$. The effect of strain on $\gamma_{\rm rad}$ is plotted as the yellow area in Fig. 2(b) and Fig. 2(c). The predicted change in linewidth from $\gamma_{\rm rad}$ is slight and opposite to the overall trend [22,32,37]. Secondly, to analyze γ_{KK-KK}, we employ the recently reported effective deformation potential model of 1L TMDCs [19]. We consider the strain-induced change in the KK exciton reduced mass, mass density of the material, sound velocity, and the related phonon frequencies [20,32,38]. We find that γ_{KK-KK} decreases by about 2 (2)% per % strain for WSe$_2$ (WS$_2$), corresponding to a decrease of less than 1 meV at the highest strain achieved, plotted as the orange area in Fig. 2(b) [Fig. 2(c)] [22]. The effect of strain on γ_{KK-KK}, as well as on $\gamma_{\rm rad}$, is clearly not sufficient to account for the significant reduction observed in the linewidths [orange lines in Fig. 2(b) and Fig. 2(c)].

We thus infer that influence of strain on γ_{KK-KQ} must account for the majority of the decrease in linewidth in both WSe$_2$ and WS$_2$. We propose that the origin of the strong strain dependence of γ_{KK-KQ} arises from the near degeneracy of the KK and KQ excitons, so that slight shifts in the relative positions of the valleys can have a dramatic impact on scattering rates. In fact, the energy separation between the KQ and KK states, E_{KQ-KK}, is expected to increase due to weaker (stronger) coupling between the orbitals contributing to the K (Q) point of the CB under tensile strain [24–27,39]. Such a shift in the relative energies of the states can lead to a rapid decrease in the scattering rate due to a reduction in the density of available final states in the scattering process [24]. We show this effect schematically in Fig. 2(d). Here we develop a model to analyze the strain dependence of γ_{KK-KQ}. We must first consider the strain dependence of E_{KQ-KK}. Writing the contributions to the exciton energy in terms of

shifts of the band separation and shifts of the exciton binding energies under strain ϵ, we have

$$
\begin{aligned}
E_{KQ-KK}(\epsilon) &= E_{KQ}(\epsilon) - E_{KK}(\epsilon) \\
&= E_{KQ-KK}(0) + \Delta E_{KQ}^{\rm quasiparticle}(\epsilon) \\
&\quad - \Delta E_{KQ}^{\rm binding}(\epsilon) - \Delta E_{KK}(\epsilon).
\end{aligned}
\tag{1}
$$

Here $E_{KQ}(\epsilon)$ and $E_{KK}(\epsilon)$ are the strain-dependent energies of the KQ and KK excitons, respectively. $\Delta E_{KQ}^{\rm quasiparticle}(\epsilon)$, $\Delta E_{KQ}^{\rm binding}(\epsilon)$, and $\Delta E_{KK}(\epsilon)$ are the changes induced by strain in the KQ quasiparticle gap, KQ exciton binding energy, and the KK exciton energy, respectively. We evaluate these quantities for WSe$_2$ in the following manner. $\Delta E_{KK}(\epsilon) = -47$ meV/% strain is obtained directly from the experimental absorption spectra presented above. $\Delta E_{KQ}^{\rm binding}(\epsilon)$ can be estimated from the change of the KQ exciton reduced mass with strain (see SM Sec. S7 [28]); we find $\Delta E_{KQ}^{\rm binding}(\epsilon) = -6$ meV/% strain [20,32,36]. We extract $\Delta E_{KQ}^{\rm quasiparticle}(\epsilon) = 15$ meV/% strain from density functional theory (DFT) calculations in the literature [10]. Combining these results, we obtain for the strain dependence of the relative energies of indirect and direct excitons

$$
E_{KQ-KK}(\epsilon) = E_{KQ-KK}(0) + 68~{\rm meV}\frac{\epsilon}{\%}.
\tag{2}
$$

The lack of significant enhancement of the PL with strain [Fig. 1(d)] indicates that $E_{KQ-KK} \gtrsim k_B T$, where k_B and T are Boltzmann constant and room temperature, respectively. If this were not the case, an increased E_{KQ-KK} at higher strain would result in significantly more KK excitons in thermal equilibrium and thus stronger PL. This view is compatible with nearly direct-gap optical excitations in 1L WSe$_2$ and WS$_2$ at room temperature that become more direct under tensile strain (see SM Sec. S1 [28] for a discussion of the PL

intensity under strain). We note that at higher strain, γ_{KK-KQ} is expected to diminish and thus the total linewidth will be dominated by γ_{KK-KK} and γ_{rad}. Thus, we infer that they contribute in total about 20 meV to the linewidth [40] which we account for to deduce γ_{KK-KQ}. We estimate $E_{KQ-KK}(0) =$ 40 (100) meV; our model fits the strain dependent linewidth reasonably well, with γ_{KK-KQ} decreasing from 21 (9) meV to 5 (4) meV for WSe$_2$ (WS$_2$), shown as the turquoise area in Fig. 2(b) [2(c)]. A higher value for E_{KQ-KK} for WSe$_2$ than WS$_2$ is consistent with the DFT calculations, since the two materials have comparable exciton binding energies [18]. Therefore, we estimate the lowest lying indirect gaps, E_{KQ}, of unstrained 1L WSe$_2$ and WS$_2$ to be 1.71 eV and 2.10 eV, respectively (see SM Sec. S5 [28]).

B. WSe$_2$ vs WS$_2$

The material properties of WSe$_2$ and WS$_2$ show generally similar trends with strain. However, measured narrowing in linewidth is significantly larger in WSe$_2$ (18 meV, 40% of the unstrained linewidth) than in WS$_2$ (6 meV, 20% of the unstrained linewidth), both of which are much larger than the magnitude of the applied strain. This observation further supports the essence of our model that a different value of $E_{KQ-KK}(0)$ (40 meV vs 100 meV) and an increase in E_{KQ-KK} can result in decreases of γ_{KK-KQ} that are proportionally much greater than the strain and are significantly different for WSe$_2$ and WS$_2$. Similar effects were reported in conventional semiconductors, such as Ge and GaAs, when excitonic binding energies and intervalley scattering were manipulated by external pressure [41,42].

C. Linewidths of other excitons

The linewidth of the B exciton, as well as of the excited states of the A exciton, are larger than that of the A_{1s} exciton. These states lie higher in energy, enabling relaxation channels beyond those presented above. Nevertheless, we expect that the intervalley scattering rate γ_{KK-KQ} of the aforementioned excitons should also decrease with strain due to the relative shifts of the higher lying KK and KQ states. Experimentally, we do indeed observe a decrease of 24 (8) meV in the B exciton linewidth of WSe$_2$ (WS$_2$) at high strain. However, a detailed and quantitative model to explain the linewidth narrowing observed for those excitons with strain is beyond the scope of this paper [43].

VIII. STRAINED VS UNSTRAINED WSe$_2$

The overall effect of strain on 1L WSe$_2$ is presented in Fig. 3(a), in which the absorption spectra of the strained and unstrained 1L are illustrated schematically. Unstrained 1L WSe$_2$ at room temperature has a ground state A exciton at 1.67 eV with a binding energy of 315 meV and a linewidth of 42 meV, with a quasiparticle gap of 1.98 eV [blue curve in Fig. 3(a)]. 2.1% strained 1L WSe$_2$ possesses a ground state A exciton at 1.57 eV with a linewidth of 24 meV and a quasiparticle gap of 1.86 eV (red curve in Fig. 3(a)). We note that the 24 meV linewidth of the strained WSe$_2$ is significantly smaller than that of the recently reported hBN encapsulated samples, 32 to 34 meV [44]. The energy separation between the lowest
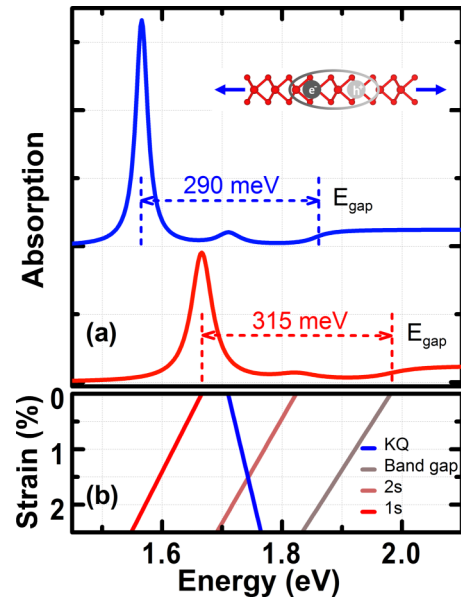

FIG. 3. (a) Schematic illustration of the absorption spectra of strained (top, offset, in blue) and unstrained (bottom, in red) 1L WSe$_2$ due to the A exciton. Vertical dashed lines denote the energies of the 1s state (left) and quasiparticle band gap (right). For clarity, only the 2s state among the excited excitonic states is shown. (b) Calculated strain-dependent positions of the A exciton 1s, 2s states, quasiparticle band gap, and KQ state.

energy direct and indirect gap states is about 145 meV larger than for the unstrained case. As a result, the ground and excited states of the A exciton are narrower and more noticeable due to weaker exciton-phonon coupling. The strain dependence of the peak positions of the A exciton 1s, 2s, quasiparticle band gap, and KQ exciton are shown in Fig. 3(b).

IX. IMPLICATIONS

Spin and valley lifetimes of excitons and electrons are expected to be longer in strained 1L WSe$_2$ and WS$_2$ since intervalley scattering is strongly suppressed. Due to the increased coherence lifetime of excitons and other tunable characteristics, strained 1Ls yield heterostructures with superior optoelectronic properties [45–49]. Moreover, higher mobility is expected from the devices made from strained 1L TMDCs due to decreased carrier-phonon intervalley scattering [20,24], as in the case of strained silicon [50].

X. SUMMARY

In summary, we have manipulated the optical signatures of the excitons of 1L WSe$_2$ and WS$_2$ via mechanical strain. We have lowered the optical band gap of 1L WSe$_2$ by 100 meV, resulting in an absorption spectrum distinct from the unstrained 1L. We have deduced that the exciton binding energy decreases by 25 meV as a result of lower exciton reduced masses, implying a decrease of 125 meV in its quasiparticle band gap. We have demonstrated that the pronounced observed narrowing in the exciton linewidth can be explained on the basis of an increased energy separation between the indirect (KQ) and direct (KK) gaps, suppressing

the phonon-induced intervalley scattering. Our results suggest that, compared to WS$_2$, WSe$_2$ has a smaller indirect-direct gap separation. As a result, a larger portion of the excitonic linewidth in 1L WSe$_2$ is due to intervalley scattering, and the *A* exciton linewidths reach the same value of 24 meV at high strain. Further studies in a regime of still higher mechanical strain [40,51] should not only yield stronger tuning of energies but also lead to further insight into the scattering and many-body physics of 2D excitons.

[1] A. Chernikov, T. C. Berkelbach, H. M. Hill, A. Rigosi, Y. Li, B. Aslan, D. R. Reichman, M. S. Hybertsen, and T. F. Heinz, Phys. Rev. Lett. **113**, 076802 (2014).

[2] K. He, N. Kumar, L. Zhao, Z. Wang, K. F. Mak, H. Zhao, and J. Shan, Phys. Rev. Lett. **113**, 026803 (2014).

[3] A. Chernikov, A. M. van der Zande, H. M. Hill, A. F. Rigosi, A. Velauthapillai, J. Hone, and T. F. Heinz, Phys. Rev. Lett. **115**, 126802 (2015).

[4] A. Raja, A. Chaves, J. Yu, G. Arefe, H. M. Hill, A. F. Rigosi, T. C. Berkelbach, P. Nagler, C. Schuller, T. Korn, C. Nuckolls, J. Hone, L. E. Brus, T. F. Heinz, D. R. Reichman, and A. Chernikov, Nat. Commun. **8**, 15251 (2017).

[5] A. V. Stier, N. P. Wilson, G. Clark, X. D. Xu, and S. A. Crooker, Nano Lett. **16**, 7054 (2016).

[6] G. Gupta, S. Kallatt, and K. Majumdar, Phys. Rev. B **96**, 081403 (2017).

[7] A. V. Stier, N. P. Wilson, K. A. Velizhanin, J. Kono, X. Xu, and S. A. Crooker, Phys. Rev. Lett. **120**, 057405 (2018).

[8] D. Lloyd, X. H. Liu, J. W. Christopher, L. Cantley, A. Wadehra, B. L. Kim, B. B. Goldberg, A. K. Swan, and J. S. Bunch, Nano Lett. **16**, 5836 (2016).

[9] H. J. Conley, B. Wang, J. I. Ziegler, R. F. Haglund, S. T. Pantelides, and K. I. Bolotin, Nano Lett. **13**, 3626 (2013).

[10] S. B. Desai, G. Seol, J. S. Kang, H. Fang, C. Battaglia, R. Kapadia, J. W. Ager, J. Guo, and A. Javey, Nano Lett. **14**, 4592 (2014).

[11] R. Schmidt, I. Niehues, R. Schneider, M. Druppel, T. Deilmann, M. Rohlfing, S. M. de Vasconcellos, A. Castellanos-Gomez, and R. Bratschitsch, 2D Mater. **3**, 021011 (2016).

[12] J. T. Ji, A. M. Zhang, T. L. Xia, P. Gao, Y. H. Jie, Q. Zhang, and Q. M. Zhang, Chin. Phys. B **25**, 077802 (2016).

[13] K. He, C. Poole, K. F. Mak, and J. Shan, Nano Lett. **13**, 2931 (2013).

[14] J. O. Island, A. Kuc, E. H. Diependaal, R. Bratschitsch, H. S. J. van der Zant, T. Heine, and A. Castellanos-Gomez, Nanoscale **8**, 2589 (2016).

[15] G. H. Ahn, M. Amani, H. Rasool, D. H. Lien, J. P. Mastandrea, J. W. Ager, M. Dubey, D. C. Chrzan, A. M. Minor, and A. Javey, Nat. Commun. **8**, 608 (2017).

[16] I. Niehues, R. Schmidt, M. Druppel, P. Marauhn, D. Christiansen, M. Selig, G. Berghauser, D. Wigger, R. Schneider, L. Braasch, R. Koch, A. Castellanos-Gomez, T. Kuhn, A. Knorr, E. Malic, M. Rohlfing, S. Michaelis de Vasconcellos, and R. Bratschitsch, Nano Lett. **18**, 1751 (2018).

[17] B. Aslan, I. M. Datye, M. J. Mleczko, K. Sze Cheung, S. Krylyuk, A. Bruma, I. Kalish, A. V. Davydov, E. Pop, and T. F. Heinz, Nano Lett. **18**, 2485 (2018).

[18] A. Kormanyos, G. Burkard, M. Gmitra, J. Fabian, V. Zolyomi, N. D. Drummond, and V. Fal'ko, 2D Mater. **2**, 022001 (2015).

[19] Z. H. Jin, X. D. Li, J. T. Mullen, and K. W. Kim, Phys. Rev. B **90**, 045422 (2014).

[20] M. Hosseini, M. Elahi, M. Pourfath, and D. Esseni, IEEE Trans. Electron Devices **62**, 3192 (2015).

[21] X. Li, J. T. Mullen, Z. Jin, K. M. Borysenko, M. Buongiorno Nardelli, and K. W. Kim, Phys. Rev. B **87**, 115418 (2013).

[22] M. Selig, G. Berghauser, A. Raja, P. Nagler, C. Schuller, T. F. Heinz, T. Korn, A. Chernikov, E. Malic, and A. Knorr, Nat. Commun. **7**, 13279 (2016).

[23] K. Kaasbjerg, K. S. Thygesen, and K. W. Jacobsen, Phys. Rev. B **85**, 115317 (2012).

[24] M. Hosseini, M. Elahi, M. Pourfath, and D. Esseni, Appl. Phys. Lett. **107**, 253503 (2015).

[25] C. E. P. Villegas and A. R. Rocha, J. Phys. Chem. C **119**, 11886 (2015).

[26] S. H. Rhim, Y. S. Kim, and A. J. Freeman, Appl. Phys. Lett. **107**, 241908 (2015).

[27] Moh. Adhib Ulil Absor, H. Kotaka, F. Ishii, and M. Saito, Phys. Rev. B **94**, 115131 (2016).

[28] See Supplemental Material at http://link.aps.org/supplemental/10.1103/PhysRevB.98.115308 for which includes Refs. [52–66], details on sample fabrication and optical measurements, additional strain-dependent optical spectra, strain dependence of the parameters used in this paper, comments on the following: indirect gap of WSe$_2$, effect of hBN encapsulation on the linewidth, orientation dependence of strain, built-in and temperature-driven strain.

[29] C. D. Zhang, Y. X. Chen, A. Johnson, M. Y. Li, L. J. Li, P. C. Mende, R. M. Feenstra, and C. K. Shih, Nano Lett. **15**, 6494 (2015).

[30] W. T. Hsu, L. S. Lu, D. Wang, J. K. Huang, M. Y. Li, T. R. Chang, Y. C. Chou, Z. Y. Juang, H. T. Jeng, L. J. Li, and W. H. Chang, Nat. Commun. **8**, 929 (2017).

[31] J. Lindlau, C. Robert, V. Funk, J. Förste, M. Förg, L. Colombier, A. Neumann, E. Courtade, S. Shree, T. Taniguchi, K. Watanabe, M. M. Glazov, X. Marie, B. Urbaszek, and A. Högele, arXiv:1710.00988.

[32] M. Feierabend, A. Morlet, G. Berghauser, and E. Malic, Phys. Rev. B **96**, 045425 (2017).

[33] H. L. Shi, H. Pan, Y. W. Zhang, and B. I. Yakobson, Phys. Rev. B **87**, 155304 (2013).

[34] T. Berkelbach (private communication).

[35] D. Le, A. Barinov, E. Preciado, M. Isarraraz, I. Tanabe, T. Komesu, C. Troha, L. Bartels, T. S. Rahman, and P. A. Dowben, J. Phys. Condens. Matter **27**, 182201 (2015).

[36] B. Amin, T. P. Kaloni, and U. Schwingenschlogl, RSC Adv. **4**, 34561 (2014).

[37] G. Moody, C. K. Dass, K. Hao, C. H. Chen, L. J. Li, A. Singh, K. Tran, G. Clark, X. D. Xu, G. Berghauser, E. Malic, A. Knorr, and X. Q. Li, Nat. Commun. **6**, 8315 (2015).

[38] A. M. Dadgar, D. Scullion, K. Kang, D. Esposito, E.-H. Yang, I. P. Herman, M. A. Pimenta, E.-J. G. Santos, and A. N. Pasupathy, Chem. Mater. **30**, 5148 (2018).

[39] C. H. Chang, X. F. Fan, S. H. Lin, and J. L. Kuo, Phys. Rev. B **88**, 195420 (2013).

[40] B. Aslan, Y. Yu, L. Cao, and M. Brongersma (unpublished).

[41] A. R. Goni, A. Cantarero, K. Syassen, and M. Cardona, Phys. Rev. B **41**, 10111 (1990).

[42] G. H. Li, A. R. Goni, K. Syassen, and M. Cardona, Phys. Rev. B **49**, 8017 (1994).

[43] I. Bernal-Villamil, G. Berghauser, M. Selig, I. Niehues, R. Schmidt, R. Schneider, P. Tonndorf, P. Erhart, S. M. de Vasconcellos, R. Bratschitsch, A. Knorr, and E. Malic, 2D Mater. **5**, 025011 (2018).

[44] F. Cadiz, E. Courtade, C. Robert, G. Wang, Y. Shen, H. Cai, T. Taniguchi, K. Watanabe, H. Carrere, D. Lagarde, M. Manca, T. Amand, P. Renucci, S. Tongay, X. Marie, and B. Urbaszek, Phys. Rev. X **7**, 021026 (2017).

[45] J. Lee, J. S. Huang, B. G. Sumpter, and M. Yoon, 2D Mater. **4**, 021016 (2017).

[46] W. Wei, Y. Dai, C. W. Niu, and B. B. Huang, Sci. Rep. **5**, 17578 (2015).

[47] D. M. Guzman and A. Strachan, J. Appl. Phys. **115**, 243701 (2014).

[48] H. Kumar, D. Q. Er, L. Dong, J. W. Li, and V. B. Shenoy, Sci. Rep. **5**, 10872 (2015).

[49] S. Pak, J. Lee, Y. W. Lee, A. R. Jang, S. Ahn, K. Y. Ma, Y. Cho, J. Hong, S. Lee, H. Y. Jeong, H. Im, H. S. Shin, S. M. Morris, S. Cha, J. I. Sohn, and J. M. Kim, Nano Lett. **17**, 5634 (2017).

[50] M. V. Fischetti and S. E. Laux, J. Appl. Phys. **80**, 2234 (1996).

[51] S. Bertolazzi, J. Brivio, and A. Kis, ACS Nano **5**, 9703 (2011).

[52] B. Aslan, Probing Transition Metal Dichalcogenides via Strain-Tuned and Polarization-Resolved Optical Spectroscopy, Ph.D. thesis, Columbia University, 2017.

[53] T. Jiang, R. Huang, and Y. Zhu, Adv Funct Mater **24**, 396 (2014).

[54] H. L. Zeng, G. B. Liu, J. F. Dai, Y. J. Yan, B. R. Zhu, R. C. He, L. Xie, S. J. Xu, X. H. Chen, W. Yao, and X. D. Cui, Sci. Rep. **3**, 1608 (2013).

[55] W. J. Zhao, R. M. Ribeiro, M. L. Toh, A. Carvalho, C. Kloc, A. H. C. Neto, and G. Eda, Nano Lett. **13**, 5627 (2013).

[56] W. Zhao, Z. Ghorannevis, L. Chu, M. Toh, C. Kloc, P.-H. Tan, and G. Eda, ACS Nano **7**, 791 (2013).

[57] T. C. Berkelbach, M. S. Hybertsen, and D. R. Reichman, Phys. Rev. B **88**, 045318 (2013).

[58] A. Polimeni, A. Patane, M. Grassi Alessi, M. Capizzi, F. Martelli, A. Bosacchi, and S. Franchi, Phys. Rev. B **54**, 16389 (1996).

[59] A. Ait-Ouali, R. Y. F. Yip, J. L. Brebner, and R. A. Masut, J. Appl. Phys. **83**, 3153 (1998).

[60] A. Ait-Ouali, J. L. Brebner, R. Y. F. Yip, and R. A. Masut, J. Appl. Phys. **86**, 6803 (1999).

[61] F. Yang, M. Wilkinson, E. J. Austin, and K. P. O'Donnell, Phys. Rev. Lett. **70**, 323 (1993).

[62] O. A. Ajayi, J. V. Ardelean, G. D. Shepard, J. Wang, A. Antony, T. Taniguchi, K. Watanabe, T. F. Heinz, S. Strauf, X. Y. Zhu, and J. C. Hone, 2D Mater. **4**, 031011 (2017).

[63] Z. Y. Huang, C. Y. He, X. Qi, H. Yang, W. L. Liu, X. L. Wei, X. Y. Peng, and J. X. Zhong, J. Phys. D Appl. Phys. **47**, 075301 (2014).

[64] M. K. L. Man, S. Deckoff-Jones, A. Winchester, G. S. Shi, G. Gupta, A. D. Mohite, S. Kar, E. Kioupakis, S. Talapatra, and K. M. Dani, Sci. Rep. **6**, 20890 (2016).

[65] C. Yelgel, O. C. Yelgel, and O. Gulseren, J. Appl. Phys. **122**, 065303 (2017).

[66] C. R. Zhu, G. Wang, B. L. Liu, X. Marie, X. F. Qiao, X. Zhang, X. X. Wu, H. Fan, P. H. Tan, T. Amand, and B. Urbaszek, Phys. Rev. B **88**, 121301 (2013).